ELSEVIER

Journal of Hydrology 254 (2001) 67–81

Journal of Hydrology

www.elsevier.com/locate/jhydrol

Simulating unsaturated flow and transport in a macroporous soil to tile drains subject to an entrance head: model development and preliminary evaluation

A. Kohler[a], K.C. Abbaspour[b,*], M. Fritsch[c], M. Th. van Genuchten[d], R. Schulin[e]

[a]*Swiss Federal Institute of Technology, Department for Land and Water Management, ETH Hönggerberg, 8093 Zurich, Switzerland*
[b]*Swiss Federal Institute for Environmental Science and Technology (EAWAG), 8600 Dübendorf, Switzerland*
[c]*Bob Partners GmbH, Blaufahnenstrasse 14, CH-8093 Zurich, Switzerland*
[d]*U.S. Salinity Laboratory, USDA, ARS, 450 West Big Spring Road, Riverside, CA, 92507 USA*
[e]*Swiss Federal Institute of Technology, Department of Soil Protection, Grabenstrasse 3, 8952 Schlieren, Switzerland*

Received 6 October 2000; revised 8 May 2001; accepted 3 July 2001

Abstract

Accurate prediction of water flow and chemical transport in agricultural soil profiles requires the use of a simulation model that considers the most important physical, hydrological and chemical processes. Two important flow-related processes in tile-drained field systems are macropore flow and water discharge from the tile drains. To better account for these two processes, we extended an existing two-dimensional model (SWMS_2D) by adding a macropore flow component as well as a Hooghoudt type boundary condition that considers the presence of an entrance head at the tile drain. The macropore component is necessary to account for water and solutes short-circuiting the soil matrix, while the drainage entrance head is needed to account for the contraction of streamlines around the drains, a feature that causes delayed discharge. The applicability of the new model to a landfill problem was examined. The simulation results, which included water flow and solute transport, compared well with other models.

Keywords: Unsaturated soil; Preferential flow and transport; Macroporous soil; Tile drain; Entrance head; Modeling

1. Introduction

The gradual contamination of surface and subsurface water resources has important social, environmental, economic, and political repercussions. Although public awareness about environmental issues has increased sharply over the past two decades, many situations and practices keep contributing to contamination of our soil and water resources. These include agricultural management practices such as fertilization and pesticide applications, the use of septic fields, and the construction of landfills, radioactive waste disposal sites, wastewater and sewage lagoons, and mine tailing embankments. Reliable analyses of these contamination problems require models that account for the most important physical, hydrological, and chemical processes. The focus of this study is on two important flow processes in tile-drained agricultural fields: preferential flow and discharge through tile drains.

The Swiss Federal Office of Environment, Forest and Landscape (FOEFL, 1997) estimated that the

* Corresponding author. Tel.: +41-1-823-5359; fax: +41-1-823-5375.
E-mail address: abbaspour@eawag.ch (K.C. Abbaspour).

0022-1694/01/$ - see front matter
PII: S0022-1694(01)00499-1

Nomenclature

a	Distance between the centre of the soil aggregates to the centre of the pores (l)
A	Coefficient of Hooghoudt equation (t^{-1})
B	Coefficient of Hooghoudt equation ($l^{-1}\,t^{-1}$)
c	Solution concentration (ml^{-3})
c_s	Concentration of the sink term (ml^{-3})
C	Coefficient of Hooghoudt equation
C_d	Drain coefficient
d	Number of days after a 5 mm rainfall event
D_{ij}	Dispersion coefficient tensor ($l^2\,t^{-1}$)
dh_i	Difference between the water potentials of micro- and macro-node i (l)
dz_i	Vertical distance between macro-nodes $(i-1)$ and i (l)
E	Effective porosity of the macro-domain
E_a	Actual evapotranspiration ($l\,t^{-1}$)
E_{pot}	Potential evapotranspiration ($l\,t^{-1}$)
h	Pressure head (l)
h_T	Elevation of the groundwater table above the tile depth, midway between the drains (l)
h_e	Entrance head (l)
$K(h)$	Unsaturated hydraulic conductivity ($l\,t^{-1}$)
K_{ij}^A	Components of a dimensionless anisotropy tensor K^A
K_s	Saturated hydraulic conductivity ($l\,t^{-1}$)
$K_{s,mac}$	Saturated hydraulic conductivity of the macropore ($l\,t^{-1}$)
K_{drain}	Adjusted conductivity of the elements surrounding a drain ($l\,t^{-1}$)
L_c	Characteristic length representing average spacing pf macropores (l)
m	$1-1/n$
n	van Genuchten shape parameter
n^*	Empirical exponent accounting for the pore size
q	Water flux ($l\,t^{-1}$)
$Q_{mac,i}$	Water flow from macro-node i down to macro-node $i+1$ (t^{-1})
Q_e	Exchange flow between a macro-node and a corresponding micro-node (t^{-1})
s	Absorbed concentration
S	Sink term (t^{-1})
S_e	Effective water saturation
t	Time (t)
x_j	Spatial coordinates (l)
z	Vertical spatial coordinate (l)
α	van Genuchten shape parameter (l^{-1})
β	Geometric factor
ϵ	Empirical factor
γ_w	Zero-order rate constants for the liquid phase ($ml^{-3}\,t^{-1}$)
γ_s	Zero-order rate constants for the solid phase ($ml^{-3}\,t^{-1}$)
μ_s	First-order rate constants for solutes in solid phases (t^{-1})
μ_w	First-order rate constant for solutes in the liquid phases (t^{-1})
θ	Volumetric water content ($l^3\,l^{-3}$)
θ_r	Residual water content ($l^3\,l^{-3}$)
θ_s	Saturated water contents ($l^3\,l^{-3}$)
θ_{mac}	Water content of macropores ($l^3\,l^{-3}$)
ρ	Soil bulk density (ml^{-3})

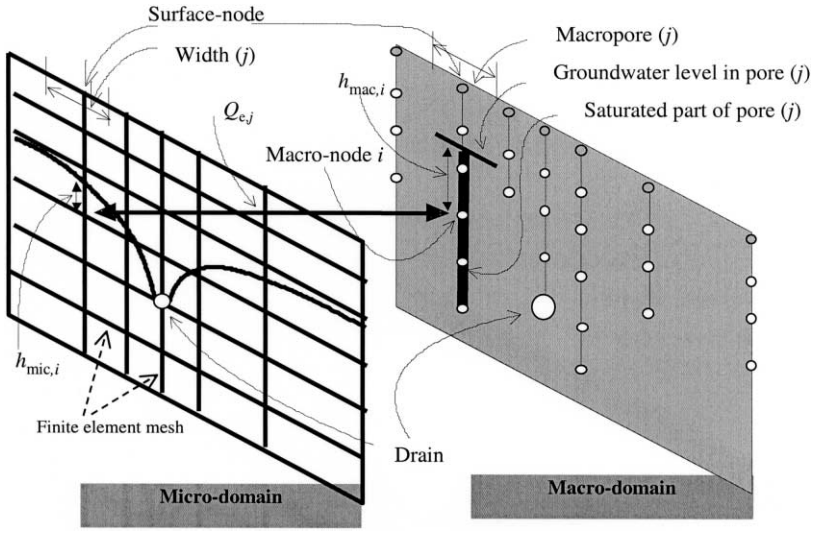

Fig. 1. Illustration of the two flow domains used in the extended M-2D model.

annual total nitrogen loss in catchments of the Rhine to be as high as 50 kg ha^{-1}. Environmentalists often identify drained lands as a major source of surface water quality problems (Evans et al., 1989). These concerns are supported by a recent study by Stamm (1997) who found that solute leached rapidly through a tile-drained field soil and ended up quickly in a creek that captured the drainage water. Even such sorbing constituents as phosphorus and ammonium appeared quickly in the drain water after application to the field. This rapid transport to the drains was attributed to the presence of preferential flow paths. Similar observations of preferential flow and transport in tile-drained fields were also made by Richard and Steenhuis (1988); Klavidko et al. (1991); Mohanty et al. (1997, 1998); and Lennartz et al. (1999), among many others.

In order to more effectively use simulation models for improving farming operations and fertilization practices, minimizing tile-drain losses of nutrients and pesticides, and optimising drainage design and water table management, it is essential that these models account for the most important flow and transport processes. Van Genuchten and Wierenga (1976) proposed a two-domain model to describe solute displacement in a structured soil under steady-state flow condition. They partitioned the water phase into a mobile (macropore) region subject to convective-dispersive transport, and an immobile, quasi-stagnant liquid (micropore) region that was coupled to the mobile region by diffusive solute exchange following first-order kinetics. Gerke and van Genuchten (1993) later extended this approach to transient water flow by applying Richards equations to both regions and coupling them in analogy to solute transport by using a first-order rate equation. Jarvis et al. (1991) developed a similar model, MACRO, to describe water flow and transport in macroporous soils. Contrary to Gerke and van Genuchten (1993), they considered water movement in the macropore region to be a non-capillary laminar flow process driven by gravity only, and assumed solute transport in the macropores to be a purely convective process. Van Genuchten and Sudicky (1999) reviewed these and other conceptualisations of macropore flow in soils and unsaturated fractured rocks.

Jarvis (1991) included tile drainage in their one-dimensional MACRO model by means of a special boundary condition. Water flow to the drains was described using the seepage potential theory of Youngs (1980) in which for each layer of the one-dimensional column a lateral loss to the drain was estimated. Loss of solute to the drains was calculated assuming complete mixing within a flow domain in the horizontal dimension.

The objectives of this study were to add a macropore

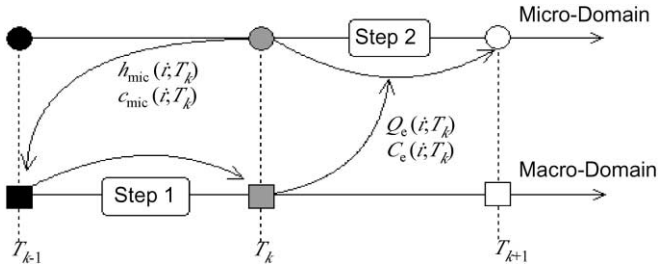

Fig. 2. Steps in numerical procedure to solve the water flow and solute transport equations. In step 1, the macropore flow and the interaction between the flow regions are calculated. In step 2, the calculated flow is used as a boundary condition for the next time step of the micro-domain.

flow component and a tile drain boundary condition to the SWMS_2D two-dimensional variably-saturated flow/transport model of Simunek et al. (1994), in order to describe water flow and solute transport in a tile-drained soil exhibiting preferential flow. In this paper we introduce the new model, henceforth referred to as M-2D, discuss an example comparing M-2D simulation results with those obtained with SWMS_2D and MACRO, and present calibration of the model for the simulation of hourly discharge through a landfill in Switzerland. The calibrated model was then used to simulate electrical conductivity of the discharge through the landfill. In a second paper (Abbaspour et al., 2001) we used the new model to analyse an experimental data set collected at a tile-drained agricultural field north of Zürich, Switzerland.

2. Description of M-2D

2.1. General description

Fig. 1 depicts the two domains of the M-2D model. The micropore domain (further referred to as the micro-domain) represents the soil matrix in which water flow is governed by the Richards equation and solute transport by Fickian-based convection-dispersion equation, respectively. The macropore domain (macro-domain) in Fig. 1 represents surface-connected cracks and macropores in which water flow within the macropores occurs one-dimensionally as non-capillary, laminar flow and in which solute transport is purely convective. Mohanty et al. (1998) from their comprehensive study of the preferential transport of nitrate to a tile drain in an intermittent flood-irrigated field in New Mexico concluded that preferential flow intercepted by a tile drain was generated in close proximity of the drain and was essentially oriented vertically. A dye infiltration test at our study site also showed that in a flat drained field and in a flat landfill the mechanism of preferential flow and transport was directed vertically downward. Hence, consideration of a two-dimensional flow within macropores, while adding considerable computational effort in the program, did not seem to be warranted.

As depicted in Fig. 1, the macro-domain has the same geometry as the micro-domain. A macropore is assumed to consist of a sequence of macropore nodes (macro-nodes) that extend vertically from a surface micropore node (micro-node) down to a desired depth. Each macro-node coincides with a certain micro-node, but not vice-versa (i.e., not all micropores are close to or connected with a macropore). The width of a macro-node is assumed to be equal to the width of the corresponding micro-node at the soil surface. After the finite element grid of the system is implemented, the user determines if a certain location of the micropore domain should correspond to a macropore domain, for example near a drain.

Following Gerke and van Genuchten (1993), exchange of water between a micro-node and corresponding macro-node is calculated based on the pressure head difference between the two nodes. We assume that the macro-node has a pressure head equal to the height of the water column in the macropore above that node. The surface nodes of macropores can also store surface water. If the micro-domain is not able to absorb all of the applied water at the surface, as indicated by a specified parameter h_{CritS}, excess water is

directed to the surface macro-nodes from which water may enter a macropore.

Within the soil profile we have the same flow exchange mechanism as for the surface nodes. If the pressure head at a certain micro-node reaches a critical value of close to saturation (specified by the parameter h_{CritS}), and a corresponding macro-node exists that is not already saturated, water will flow from the micro-node to the macro-node according to an interaction term to be discussed later.

The numerical procedure for successive calculation of flow and transport between the micro- and macro-domains is depicted in Fig. 2. Assuming that the micro-domain was solved for time T_k, the model calculates flow and transport in the macro-domain as follows. During step 1, pressure heads of the micro-domain are compared to those of the macro-domain and the interaction term for flow between the two flow domains is calculated. Based upon the actual water contents in the macropores and the interaction term, water flow and solute transport for time step T_{k-1} to T_k are calculated for each macropore. During step 2, flow and transport in the micro-domain are solved for the next time step from T_k to T_{k+1}. During this step the interaction term between the two flow domains, which was calculated in step 1, is treated as a boundary condition by means of prescribed in- or outflow rates from the corresponding micro-nodes.

2.2. Variably-saturated flow

2.2.1. Micropore domain

In SWMS_2D (Simunek et al., 1994), water flow in a two-dimensional, isothermal, variably-saturated, rigid porous medium is described with the following form of the Richards equation:

$$\frac{\partial\theta}{\partial t} = \frac{\partial}{\partial x_i}\left[k(h)\left(K_{ij}^{A}\frac{\partial h}{\partial x_j} + K_{ij}^{A}\right)\right] - S \tag{1}$$

where θ is the volumetric water content, h is the pressure head, S is a sink term, x_j ($j = 1,2$) are the spatial coordinates, t is time, K_{ij}^{A} are components of a dimensionless anisotropy tensor K^{A}, and $K(h)$ is the unsaturated hydraulic conductivity function.

Soil hydraulic properties are described using van Genuchten's model (van Genuchten, 1980) for the water retention function:

$$S_{\mathrm{e}}(h) = \frac{\theta(h) - \theta_{\mathrm{r}}}{\theta_s - \theta_{\mathrm{r}}} = \frac{1}{(1 + |\alpha h|^{n})^{m}} \quad h < 0 \tag{2}$$

$$\theta(h) = \theta_S \qquad h \geq 0 \tag{3}$$

and the van Genuchten-Mualem model (Mualem, 1976) for the hydraulic conductivity function:

$$K(h) = \begin{cases} K_S S_{\mathrm{e}}^{0.5}(1 - (1 - S_{\mathrm{e}}^{1/m})^{m})^{-2} & h < 0 \\ K_S & h \geq 0 \end{cases} \tag{4}$$

in which α and n are shape parameters, S_{e} is effective saturation, $m = 1 - 1/n$, θ_{r} and θ_s are the residual and saturated water contents, respectively, and K_s is the saturated hydraulic conductivity.

2.2.2. Macropore domain

Water within a macropore is assumed to move by gravitational flow from the surface node down to the bottom of the macropore. The hydraulic conductivity at each node is calculated as a function of the relative saturation of the macro-node according to:

$$K_{\mathrm{mac}}(\theta_{\mathrm{mac}}) = \begin{cases} K_{s,\mathrm{mac}}\left(\dfrac{\theta_{\mathrm{mac}}}{E}\right)^{n^{*}\prime} & 0 < \theta_{\mathrm{mac}} < \theta_{s,\mathrm{mac}} \\ K_{s,\mathrm{mac}} & 0_{\mathrm{mac}} = \theta_{s,\mathrm{mac}} \\ 0 & \theta_{\mathrm{mac}} = 0 \end{cases} \tag{5}$$

where $K_{s,\mathrm{mac}}$ is the saturated hydraulic conductivity of the macropore, θ_{mac} is the water content, E is the macroporosity of the soil (i.e., the total volume of macropores per bulk soil volume), and n^{*} is an empirical exponent reflecting the macropore size distribution. More details about the formulation of Eq. (5), or how the parameters can be measured, can be found in the manual of model MACRO (Jarvis, 1991), or in Beven and Germann (1981).

Water flow in the macro-domain is calculated by means of the following steps: (i) determination of the pressure head at each macro-node, (ii) calculation of the interaction term between micro- and macro-nodes and (iii) redistribution of water within the macropores. These steps are repeated several times within each time step of the micropore model. The time step of the macropore sub-model is prescribed by the user and kept fix during the model run.

The exchange of water between the macro- and micro-domains is calculated for each macro-node by comparing the pressure head of the macro-node with that of corresponding micro-node. The exchange rate of water, $Q_{e,i}$, between the two flow regions at macro-node i is described as proposed by Beven and Germann (1981) in analogy to Darcy's law:

$$Q_{e,i} = -K_i(h_{mic})\frac{dh_i}{L_c^2} \tag{6}$$

in which:

$$dh_i = h_{mic,i} - h_{mac,i} \tag{7}$$

where $K_i(h_{mic})$ is the hydraulic conductivity of micro-node i, and L_c is the characteristic length representing the average spacing of the macropores as well as the geometry of the macroporous system. Gerke and van Genuchten (1993) used a similar equation in their model and derived the following expression for the characteristic length:

$$L_c^2 = \frac{a^2\epsilon}{\beta} \tag{8}$$

where β is a geometric factor (equal to 3 for rectangular slabs and 15 for spherical shapes), a is the distance between the centre of the soil aggregates or soil matrix domain to the centre of the macropores, and ϵ is an empirical factor set equal to 0.4.

For some cases the exchange of water is set to zero. For example, when $dh_i < 0$, i.e., pressure head gradient is directed towards micropore i, but at the same time micropore i is saturated or macropore i is unsaturated. Also, $Q_{e,i}$ is set to zero when $dh_i > 0$, i.e., pressure head gradient is directed towards macropore i, but micropore i is unsaturated.

After calculating the water exchange rate between the two domains, the water content of each macro-node is updated using the expression:

$$\theta_{mac,new,i} = \theta_{mac,old,i} + Q_{e,i}dt \tag{10}$$

If $\theta_{mac,new,i}$, calculated in this manner exceeds the macroporosity, E_i, of macro-node i, then its value is set equal to E_i and $Q_{e,i}$ is correspondingly adjusted. Similarly, if $\theta_{mac,new,i}$, is negative, its value is set equal to zero and $Q_{e,i}$ is correspondingly reduced. The new water contents, as discussed next, are starting values for calculating water flow within the macropores.

2.2.3. Redistribution of water within macropores

Redistribution of water in the macropores is calculated in two steps. The first step involves solution of the equations:

$$\frac{\partial\theta_{mac,i}}{\partial t} = \frac{\partial K(\theta_{mac,i})}{\partial z_i} - Q_{e,i} \tag{11}$$

where $\partial\theta_{mac,i}$, represents the change in water content of macro-node i. Eq. (11) is calculated from the surface node down to the bottom node of the macropore. After solving Eq. (11), the macropores are checked for over-saturation ($\theta_{mac,i} > E_i$) and the surplus of water is redistributed from bottom to the top. Eq. (11) is solved using an implicit, iterative interval halving method (Gerald and Wheatley, 1989).

2.3. Solute transport

2.3.1. Solute transport in the micro-domain

Solute transport in the micro-domain is described by the convection-dispersion equation including source/sink terms for transformation processes that follow first- and zero-order kinetics (Simunek et al., 1994):

$$\frac{\partial\theta c}{\partial t} = \frac{\partial}{\partial x_i}\left(\theta D_{ij}\frac{\partial c}{\partial x_i}\right) - \frac{\partial q_i c}{\partial x_i} + \mu_w\theta c + \mu_s s\rho + \gamma_w\theta + \gamma_s\rho - Sc_s \tag{12}$$

where c is the solution concentration, s is the sorbed concentration, q_i is the ith component of the volumetric flux, μ_w and μ_s are first-order rate constants for solutes in the liquid and solid phases, respectively, γ_w and γ_s are zero-order rate constants for the liquid and solid phases, respectively, ρ is the soil bulk density, S is the sink term, c_s is the concentration of the sink term, and D_{ij} is the dispersion coefficient tensor.

2.3.2. Solute concentration of macro-nodes and solute exchange between domains

Solute transport within the macro-domain and between the domains is calculated by assuming a purely convective process. Water with a certain solute concentration entering a macro-node is immediately mixed with water associated with that macro-node. After mixing, water is moved down to the next macro-node as follows. First, water flow, $Q_{mac,i}$,

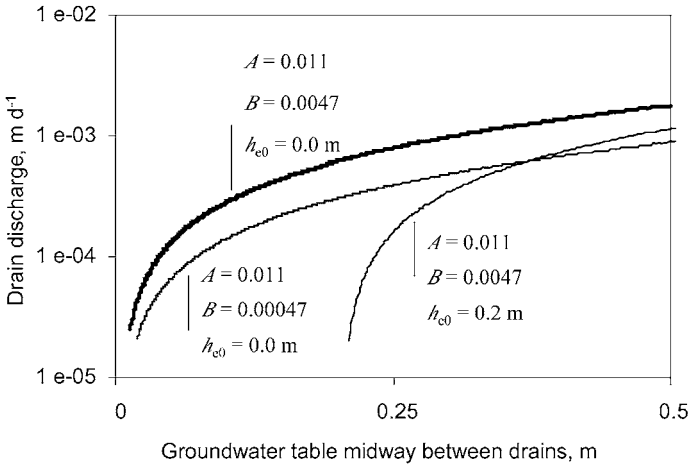

Fig. 3. Drain discharge versus groundwater table above the tile drain, midway between drain as a function of varying parameters in Hooghoudt drain boundary condition.

from macro-node i vertically downward to node $i + 1$ is calculated according to:

$$Q_{\mathrm{mac},i} = \frac{1}{dt}(\theta_{\mathrm{mac,old},i} - \theta_{\mathrm{mac,new},i}) + Q_{\mathrm{mac},(i-1)} + Q_{\mathrm{e},i} \tag{13}$$

The procedure starts at the surface node and proceeds downward. Using the water fluxes calculated in this manner for each macro-node, a solute mass balance is carried out next. To perform the mass balance, the concentration of the exchange flow is set equal to the concentration of the macro-node if the exchange flow is directed toward the micropore, and set equal to the concentration of the micro-node if the flow is directed toward the macropore. The system of solute mass balance equations for all nodes of a macropore is subsequently solved using Gaussian elimination.

2.4. Hooghoudt boundary condition

The traditional way to model an ideal drain in a field-scale finite element model is to represent the drain as a node with a system-dependent boundary condition in which the pressure head is set to zero when the drain node is saturated, and the flux is set to zero when the drain node is unsaturated. This approach does not account for the contraction of the streamlines near the drain, the presence of a non-uniform pressure along the drain boundary, and the presence of an entrance head around the drain. Entrance head is the minimum head that is required to initiate flow in a drain. A comparison of discharges calculated with the analytical solution of Kirkham (1949) and numerically simulated drain flows showed that the discrepancy could be substantial. Fipps and Skaggs (1986) demonstrated that only a model representing the drainage tube at sufficiently high resolution and in its full shape would lead to accurate estimation of the groundwater table and the drainage discharge rate.

Lacking sufficient spatial resolution to explicitly describe the local non-uniformity of the flow field around and along slotted drainpipes, field-scale models usually try to account for the head loss caused by streamline convergence by invoking an empirical resistance. The dependence of this resistance on perforation sizes and arrangements, as well as on the dimensions and conductivity of the surrounding material has been theoretically analyzed by Dierickx (1980), among others. Other factors such as clogging of flow paths by particle deposition and disturbance of the soil around drain pipes or the envelope material may further add to the non-uniformity of the flow field at a drain boundary. As it is usually neither possible nor necessary to separate all these individual effects, the concept has been extended to include all other forms of resistance encountered by the flow entering a drain. This compound resistance as described in Stuyt et al. (2000) is called the ‘approach flow resistance’.

Table 1
Soil hydraulic parameters used for the MACRO and M-2D model comparison test

Depth [m]	α [m^{-1}]	n [-]	θ_r [-]	θ_s [-]	E [-]	K_s [m d^{-1}]	Ψ_b, h_{CritS}[a] [m]	n^* [-]	K_{mac} [m d^{-1}]	λ[b] [-]
	Parameters of M-2D									
			Parameters of MACRO							
0 – 0.3	10	2	0.2	0.5	0.01	2	-0.1	1	48	1
0.3 – 0.8	10	2	0.45	0.5	0.01	0.005	-0.1	1	48	1
0.8 – 1.5	10	2	0.45	0.5	0.01	0.6	-0.1	1	48	1

[a] Ψ_b = boundary soil water tension in the MACRO which is similar to h_{CritS} in M-2D.
[b] λ = Brooks and Corey water retention shape factor set equal to $(n - 1)$.

Simunek et al. (1994) represented drains in the SWMS_2D code as single nodes with a system-dependent boundary condition, while accounting for approach flow resistance in the entrance conditions by adjusting the conductivity of the finite elements surrounding the drainage node according to the equation:

$$K_{drain} = K_S C_d \quad (14)$$

where K_{drain} is the adjusted conductivity of the elements surrounding the drain, K_s is the actual hydraulic conductivity of the elements surrounding the drain, and C_d (<1) is a coefficient that depends on the diameter of the drain and the dimensions of the surrounding elements. This approach enables SWMS_2D to describe the hydraulic behaviour of ideal drains accurately. An ideal drain is defined in this paper as a drain with a homogenous flow field

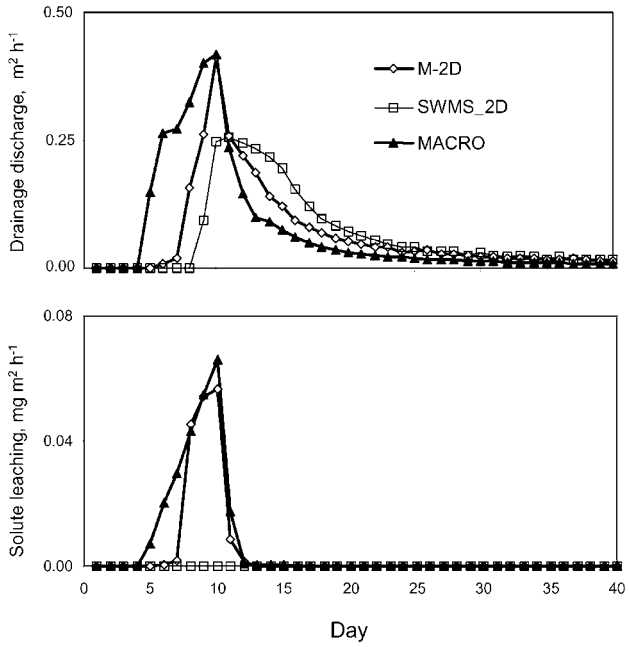

Fig. 4. A comparison of the simulated drainage outflow and the solute leaching rate between M-2D, MACRO, and SWMS_2D.

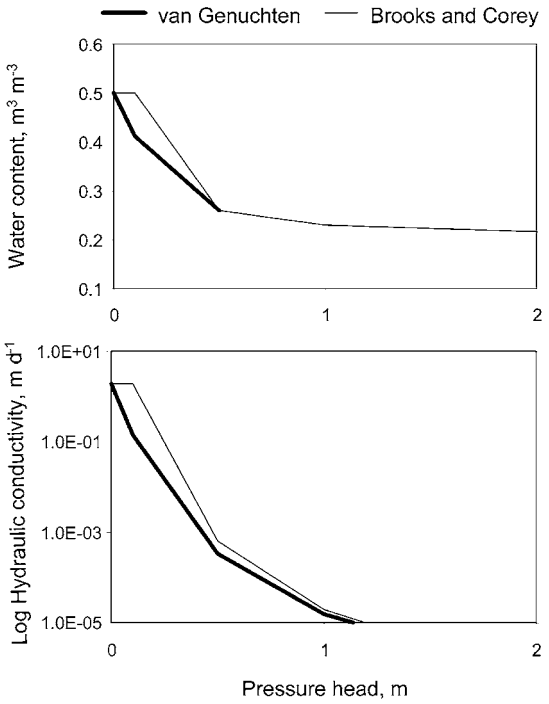

Fig. 5. Water retentions and flow curves based on Brooks and Coery and van Genuchten formulations used to compare M-2D with MACRO.

around and along the drainpipe. Although the reduction factor C_d accounts for the contraction of the flow field around the drainage pipe, it may not account for the typically non-uniform entrance head of non-ideal drains.

In a recent field study (Kohler, 2000) we studied the performance of a field tile-drainage system by measuring the groundwater drawdown during periods of high groundwater tables. We found that the field drains were subjected to relatively large entrance heads, $h_{e0} \geq 0$, that were a function of the water table height above the tile depth, midway between field drains. To be able to simulate such non-ideal drainage system with an entrance head, we implemented in the M-2D code a new type of boundary condition, further referred to as a Hooghoudt boundary condition. This condition prescribes the discharge rate q at the drain node as a function of the water table height h_T at some reference point, i.e., $q = f(h_T)$. For the experimental field studied we obtained good results using the extended Hooghoudt equation proposed by Oosterbaan et al. (1989), i.e.:

$$q = A(h_T - h_e) + B(h_T^2 - h_e^2) \quad (15)$$

in combination with the empirical finding that $h_e = Ch_T + h_{e0}$, in which C and h_{e0} are site-specific parameters, A and B are fitting constants, and where h_T was taken midway between the drains. The $q(h_T)$-function is site specific and generally should be measured. However, if no suitable $q - h_T$ data are available, the relationship may also be determined numerically by means of local high-resolution modelling of the drain performance, after which the $q(h_T)$-function can be used in field-scale models in which the drains are represented as single nodes. Note that the above empirical relationships can easily be replaced by another locally calibrated model relating drain discharge to the water table height measured at a conveniently location.

The Hooghoudt boundary condition is hence a Neumann type boundary condition in which tile drainage flow is prescribed according to the head at a reference node. The new boundary condition has the flexibility to describe a large number of drain situations since the parameters A and B in Eq. (15) can be determined empirically. This is illustrated in Fig. 3 where drain discharge is plotted as a function of the groundwater elevation midway between the drains and changing values of A, B, and h_{e0}. Notice the rise in the groundwater table needed in order to initiate the flow in the case where h_{e0} is not equal to zero.

A more accurate way to account for the drains would be to implicitly allow for flow processes in the drain by including the drain geometry in the flow domain. The only problem with this approach would be that a high-resolution discretization would be required around the drains, as already pointed out by Fipps and Skaggs (1986), which would substantially increase the number of nodes and, hence the execution time. Such a slow model would not then lend itself easily to the type of inverse analysis carried out in this study for parameter estimation.

3. Comparing M-2D and macro simulation results

We tested the macropore component of M-2D by comparing M-2D simulation results with those obtained using MACRO (1991) for a one-dimensional

test problem. The problem considers the arrival of a wetting front at the bottom of a 1.5-m long soil column. An atmospheric boundary at the soil surface and a seepage face at the bottom of the column were assumed. The set up hence resembles a free-draining lysimeter. The simulation lasted 40 days, starting with a 10-day period of precipitation at a rate of 0.01 m d^{-1}, followed by 30 days of water redistribution without any rainfall or evapo-transpiration. More detail about this test site can be found in Abbaspour et al. (2001).

The initial soil water pressure head in the column was assumed to be in hydraulic equilibrium with the bottom of the soil set at zero pressure head. The soil column was initially free of solutes, while the rainfall had a constant solute concentration of 1000 mg m^{-3}. Pertinent information regarding the soil column is listed in Table 1. The values in Table 1 were calculated by inverse modeling in a previous study by Abbaspour et al. (2001). Other parameters include dispersivity for solute transport, which was set equal to 0.1 m, and the exchange length (macropore spacing) between the flow regions, which was set equal to 0.2 m in both models.

Fig. 4 shows calculated drainage and solute leaching rates obtained with M-2D and MACRO. The same system, but without macropores, was also simulated using SWMS_2D for comparison purposes. Drainage as well as solute leaching started earlier for MACRO as compared to M-2D, but no solute leached from the column during the simulation period when SWMS_2D was used. It should be noted that MACRO uses the Brooks and Corey (1964) model of soil hydraulic characteristics, while SWMS_2D uses the van Genuchten (1980) model. Although this problem is not important for simulations under highly unsaturated conditions, it may have some effect at and near the air-entry pressure head where most of the exchange of water between the macro- and micro-domains takes place. The two hydraulic characteristic models are illustrated graphically for the first soil layer in Fig. 5. Differences between the two hydraulic functions may be important in terms of affecting the timing (initiation) and extent of a bypass flow through the macropores.

Another important difference between MACRO and M-2D may be the method in which the water exchange rate between the micro- and macropore regions is calculated. In MACRO the exchange rate is calculated as a function of the difference between the actual micropore water content and the boundary water content, whereas in M-2D water exchange is based on the pressure head differences between a micro-node and a macro-node. Geometric discretization in MACRO is also different from that in M-2D; MACRO allows only a limited number of soil layers to be considered in a simulation (set to 10 in this example), while M-2D allows essentially an unlimited number of soil layers. Given these differences, the simulation results for MACRO and M-2D in Fig. 5 are quite comparable, especially the peak tile-drainage and concentration results.

4. Testing M-2D in a field application

4.1. Field site

In a real field test of the M-2D model we simulated the hourly drainage discharge of a municipal solid waste incinerator (MSWI) bottom ash landfill near Buchs, Switzerland. Lostorf is situated in a disused gravel pit. After calibrating the model parameters for discharge, solute transport through the landfill was simulated using measured electrical conductivity of the discharge water. The landfill is 6 m deep, and a liner consisting of 0.8 m opalinous clay supporting a gravel drainage layer (0.2 m) serves to collect the leachate via high-density polyethylene (HDPE) tubing into a shaft. Two geotextiles separate the MSWI bottom ash from the drainage layer and the drainage layer from the clay liner. The surface of the landfill has not yet been covered or cultivated so there is direct contact between the atmosphere and the disposed ash.

The average yearly precipitation at the local Swiss Metrological Association (SMA) station (Buchs/Suhr, approximately 2 km west of the landfill in a comparable geographical location) for the period of 1987 to and including 1996 is 1060 mm. The average rainfall maximum occurs between May and June. The driest period is January to April. The summer rains tend to occur in storm events of high rain intensity.

We selected the above site for testing M-2D because the site has already been modelled in a previous study (Johnson et al., 2001), and this would allow us a comparison of M-2D with other models. Johnson and co-workers compared the application of several models

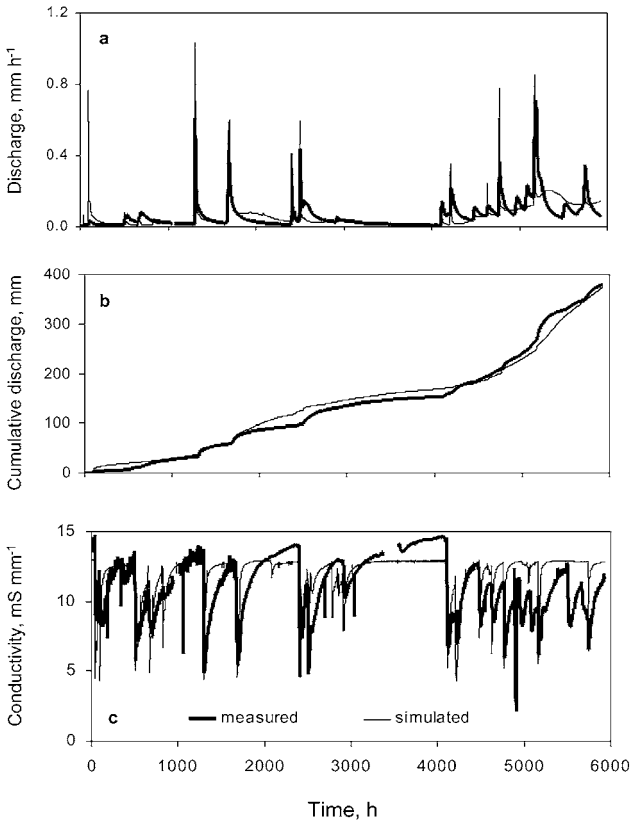

Fig. 6. Comparison of the M-2D simulation with measurements of: (a) the drainage discharge, (b) the cumulative discharge, and (c) the conductivity of the seepage water for the 1996 calibration data set.

such as a linear storage model (Huwe et al., 1994), a neural network model, HYDRUS5 (Vogel et al., 1996), and MACRO (Jarvis, 1991) for the simulation of flow through the Lostorf landfill. The hourly nature of the simulation plus the apparent existence of preferential flow makes modeling of flow and transport through the landfill especially challenging. The hourly simulation is necessary for an accurate accounting of the solute load leaching from the landfill.

4.2. Input data

Automatic registration of drainage discharge, electrical conductivity and temperature were made over the periods November 1993 to February 1993, November 1994 to November 1995, and May 1996 to December 1996. Flowtec (DI 652) instrumentation, based on changes in the magnetic field as a function of flow rate, was used to measure discharge. Conductivity and temperature were registered on-line with a combined WTW LF 196 electrode. Average values taken every second were saved to a data logger every 15 min. Precipitation measurements were made on site using a tilting-siphon rain gauge. The on-site rainfall measurements were compared to data collected by the Buchs/Suhr SMA station.

Potential evapotranspiration from the surface of the landfill was estimated using the hourly form of the FAO Penman-Monteith equation (Allen et al., 1994). Hourly values of global radiation, relative humidity, pressure, wind velocity (at 2 m) and temperature were obtained from the SMA at the Buchs/Suhr site and in addition from on-site measurements of temperature, relative humidity and wind velocity in 1996.

The actual evaporation E_a from the bare bottom ash

Table 2
The results of statistical comparisons between measured and simulated cumulative discharge for different models

Model	Calibration Objective function, g	Validation objective function, g
Neural network model[a]	7.42	15.1
Linear storage model[a]	40.4 (29.4.96–31.8.96), 7.2 (1.9.96–31.12.96)	8.2
HYDRUS5[a]	27.6	32.1
MACRO[a]	10.1	41.1
M-2D	13.1	19.4

[a] Data published in Johnson et al. (2001).

surface was estimated from the potential evapotranspiration using an empirical approach adopted from Black et al. (1969) by applying the following correction:

$$E_a = \frac{E_{pot}}{d^{0.2}} \quad (16)$$

where d is the number of days after a 5 mm rain event. Using this empirical correction approach, the total evaporation for the 1996 data sets was corrected from 3960 m^3 to 2950 m^3 and agreed well with the difference between rainfall and discharge (5860–2940 = 2950 m^3). The agreement for the 1995 data set was not as good. The evaporation estimated from rainfall, minus discharge (3490 m^3) was higher than the corrected Penman-Monteith value (3010 m^3).

Using the data set 29.4.96–31.12.96 (5928 h),

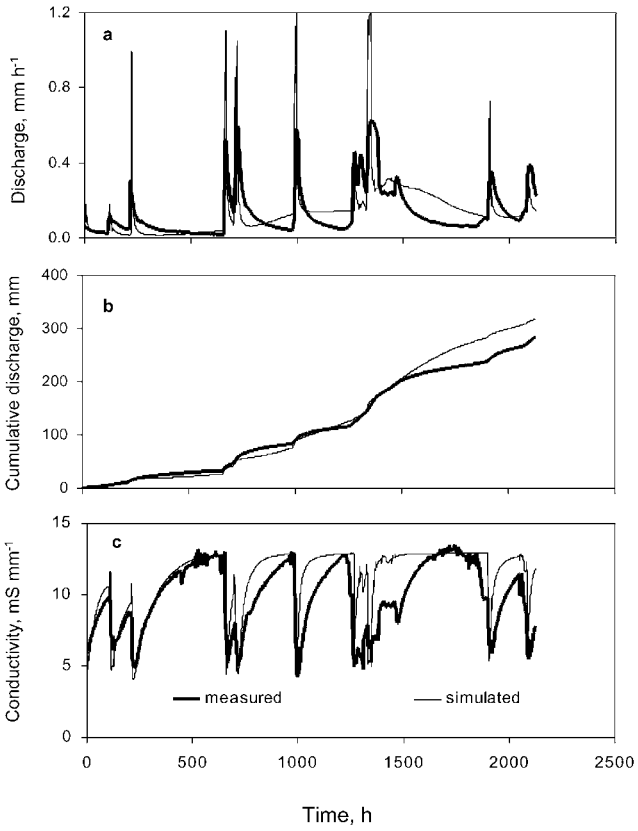

Fig. 7. Comparison of the M-2D simulation with measurements of: (a) the drainage discharge, (b) the cumulative discharge, and (c) the conductivity of the seepage water for the 1995 test data set.

M-2D was calibrated and the parameters were optimized. The model was then used to predict the discharge monitored in the period 1.12.94–7.2.95 (2125 h). Missing discharge and conductivity data caused by instrumentation failure were linearly interpolated. Such periods did not exceed 10 h and constituted less than 1% of the data sets.

4.3. Model parameterization

The initial landfill condition was expressed by a known pressure head distribution over the vertical depth of the landfill. The boundary condition at the top of the landfill was depicted as an atmospheric boundary condition with prescribed precipitation and evapotranspiration data, while at the bottom a seepage face boundary condition was imposed to simulate the drained bottom of the landfill. Initial and boundary conditions applied to the flow through the landfill were mathematically formulated as:

- Initial condition:

$$h(z,t) = h_i(z)\ t = 0 \tag{17}$$

- Atmospheric condition:

$$-k\left(\frac{\partial h}{\partial z} - 1\right) = q'(t)\ z = 0 \tag{18}$$

- Seepage face condition:

$$h(L) = 0 \text{ if } h(L) > 0, \tag{19}$$

and:

$$\frac{\partial h}{\partial z} = 0 \text{ if } h(L) < 0$$

where h_i is the initial pressure head (mm), L is the coordinate of the bottom of the soil, and $q'(t)$ is the prescribed flux (mm h^{-1}) at the surface.

Initial estimates of θ_r, θ_s, α and n were taken from unpublished laboratory desorption curves of intact MSWI bottom ash samples taken from the landfill Lostorf (Buchter, 1997). The values were $\theta_r = 0.14$ $mm^3\ mm^{-3}$, $\theta_s = 0.42\ mm^3\ mm^{-3}$, $\alpha = 0.0085$ mm^{-1} and $n = 1.18$. The SUFI program of Abbaspour et al. (1997) was used to inversely fit the unknown parameters of the micropore region α, n, θ_r, θ_s, and K_s as well as the parameters n^*, E, $K_{s,mac}$, and L_C describing the macropore region. The objective function, g, was expressed as:

$$g = \sqrt{\frac{\sum_i^m (Q - Q')_i^2}{m}} \tag{20}$$

where $m = 5928$ is the number of data points, Q is measured cumulative discharge, and Q' is simulated cumulative discharge.

4.4. Simulation results

It is important to emphasise that the simulation with the M-2D model in this study was conducted with the minimum of required information. The initial pressure head h_i, the parameters α, n, θ_r, θ_s, and K_s as well as the parameters describing the macropore region h_{CritS}, n^*, E, $K_{s,mac}$, L_C were first fitted on the measured cumulative discharge assuming a uniform distribution of the initial pressure head in the landfill.

At the beginning of the simulation period in April 1996 landfill was in a very dry state. In order to obtain values for the initial pressure head, estimates were made using the parameters obtained by the initial fitting. The flow 3000 h beyond the end of the simulation period was modelled without rainfall until the discharge rates were equal to the measured discharge at the beginning of the simulation period in April. Using the pressure head values at this stage as the initial values, the inverse estimation of the hydraulic parameters was once again performed. The results of simulations were greatly improved by the new non-uniform-initial-pressure-head data. Fig. 6a shows the measured and simulated hourly discharge as a function of time, while Fig. 6b illustrates the measured and simulated cumulative discharge. Although there are some differences in the hourly discharge rates of the measured and simulated data, the cumulative values are rather closely matched ($g = 13.1$). In Table 2, the results of simulations with M-2D are compared with other models reported by Johnson et al. (2001). The estimated values of the parameters of the micropore

region were $\alpha = 0.0015\ \mathrm{mm}^{-1}$, $n = 1.10$, $\theta_r = 0.14\ \mathrm{mm}^3\ \mathrm{mm}^{-3}$, $\theta_s = 0.45\ \mathrm{mm}^3\ \mathrm{mm}^{-3}$, and $K_s = 0.58\ \mathrm{mm\ h}^{-1}$, and of the macropore region $n^* = 5$, $E = 0.002\ \mathrm{mm}^3\ \mathrm{mm}^{-3}$, $K_{s,\mathrm{mac}} = 6\ \mathrm{mm\ h}^{-1}$, $h_{\mathrm{CritS}} = -450$ mm, and $L_c = 1$ mm.

We tested the above parameters, obtained by fitting the 1996 discharge data, by simulating the hourly discharge rates measured in 1995 (Fig. 7). The agreement between modelled and measured cumulative discharge in Fig. 7b is excellent up to about 1600 h and diverges beyond this time. The overall value of $g = 19.4$ is, however, comparable with other models (Table 2). The discrepancy in the hourly discharge rates in Fig. 7 indicates an overestimation of the fast flow component conducted by preferential flow paths, while the simulated matrix flow is not as responsive as the measured values.

As shown in Table 2 the simulation results with M-2D are comparable to those of the MACRO model published in Johnson et al. (2001). The peak flow rates simulated with M-2D are too high and too sharp compared to the measured hourly discharge, whereas the base flow from the matrix is too damped. Some reasons for these discrepancies could be the assumption of a homogeneous system for the landfill, and lack of accurate knowledge of initial and boundary conditions. For this study we assumed a homogeneous system because no information was available on system heterogeneity, and assumption of a multiplayer system would have drastically increase the computational effort.

In addition to the water flow we also simulated the solute transport by means of measured electrical conductivity of the seepage flow at the bottom of the landfill. Assuming a conductivity of $4\ \mathrm{ms\ mm}^{-1}$ for the precipitation and a conductivity of $14\ \mathrm{ms\ mm}^{-1}$ for the water stored in the matrix of the landfill, we obtained a simulated conductivity of the seepage water as shown in Fig. 6c for the calibration phase and Fig. 7c for the validation case. Since the measured conductivity of the seepage water is simulated rather well by M-2D, it can be assumed that the model describes correctly the dynamics of the water flow within the landfill system. It should be noted that the model was only fitted to the cumulative discharge and not to the solute transport information.

5. Conclusions

We extended the SWMS_2D model of Simunek et al. (1994) by adding a macropore flow component and an entrance head in the drainage boundary condition. In this paper, simulation of flow and transport through a landfill system tested the macropore component of the model.

An inverse program fitted parameters describing the flow, during calibration phase based on cumulative discharge. The calibrated model was tested using data from a previous year. Although the model over estimated the peaky dynamics of the macropore flow and under estimated the base flow through the matrix, but based on the relatively small amount of available information, the model performed satisfactorily and the discharge compared well with other models tested by Johnson et al. (2001). Simulation of the solute transport component of the model using electrical conductivity as a tracer also provided relatively good results for both calibration and validation stages.

References

Abbaspour, K.C., Kohler, A., Schulin, R., Fritsch, M., van Genuchten, M.Th., 2001. Application of a two-dimensional unsaturated flow and transport model to a macroporous agricultural field with entrance resistance to tile drains. European J. of Soil Sci., 52 (3).

Abbaspour, K.C., van Genuchten, M.T., Schulin, R., Schläppi, E., 1997, A., 1892. sequential uncertainty domain inverse procedure for estimating subsurface flow and transport parameters. Water Resour. Res. 33, 1879–1879.

Allen, R.G., Smith, M., Pereira, L.S., Perrier, A., 1994. An update for the calculation of reference evapotranspiration. ICID Bulletin, 43, 35–92.

Beven, K., Germann, P., 1981. Water flow in soil macropores. II: A combined flow model. J. Soil Sci. 32, 15–29.

Black, T.A., Gardner, W.R., Thurtell, G.W., 1969. The prediction of evaporation, drainage and soil storage for a bare soil. Soil Sci. Soc. Amer. Proc., 33, 655–660.

Brooks, R.H., Corey, A.T., 1964. Hydraulic properties of porous media. , Hydrology Paper no. 3. Colorado State University, Fort Collins, Colorado.

Buchter, B., 1997. Personal communication.

Dierickx, W., 1980. Electrolytic analogue study of the effect of openings and surrounds of various permeability on the performance of field drainage pipes. Rijksstation voor landbouwtechniek, Publication 77, Merelbeke, Belgium.

Evans, R.O., Gilliam, J.W., Skaggs, R.W., 1989. Effects of agricultural water table management on drainage water quality. Report

237 of the Water Resource Research Institute of the University of North Carolina.

Fipps, G., Skaggs, R.W., 1986. Drains as a boundary condition in finite elements. Water Resour. Res. 22, 1613–1621.

FOEFL, 1997. Verminderung des Nährstoffeintrags in die Gewässer durch Massnahmen in der Landwirtschaft. Schriftenreihe Umwelt Nr. 209 vom Bundesamt für Umwelt, Wald und Landschaft.

Gerald, C.F., Wheatley, P.O., 1989. Applied Numerical Analysis. Addison-Wesley Publishing Company, New York.

Gerke, H.H., van Genuchten, M.Th., 1993. A dual porosity model for simulating the preferential movement of water and solutes in structured porous media. Water Resour. Res. 29, 305–319.

Huwe, B., Gölz-Huwe, H., Eberhardt, J., 1994. Parameterschätzung und Madellrechnungen zum Gebietswasserhaushalt kleiner, heterogener Einzugsgebiete mit einfachen Modellkonzepten. Mitteilgn. Dtsch. Bodenkundl. Gesellsch., 74, 273–276.

Jarvis, N., 1991. MACRO A model of water movement and solute transport in macroporous soils. Department of Soil Sciences, Report and Dissertations 9, Swedish University of Agricultural Sciences, Uppsala.

Johnson, C.A., Schaap, M.G., Abbaspour, K.C., 2001. Model comparison of flow through a municipal solid waste incinerator ash landfill. J. of Hydrol. 243, 55–72.

Kirkham, D., 1949. Flow of ponded water into drain tubes overlaying an impervious layer. Am. Geophys. Union Trans. 30, 369–385.

Klavidko, E.J., van Scoyoc, G.E., Monke, E.J., Oates, K.M., Pask, W., 1991. Pesticide and nutrient movement into subsurface tile drains on a silt loam soil in Indiana. J. Environ. Qual. 20, 264–270.

Kohler, A., 2000. Investigation of water and solute outflow from macroporous agricultural fields with tile drains. PhD Dissertation, Swiss Federal Institute of Technology Zürich. In preparation.

Lennartz, B., Michaelsen, J., Wichtmann, W., Widmoser, P., 1999. Time variance analysis of preferential solute movement in a tile-drained field site. Soil Sci. Soc. Am. J. 63, 39–47.

Mohanty, B.P., Bowman, R.S., Hendrickx, J.M.H., van Genuchten, M.Th., 1997. New piece-wise continuous hydraulic functions for modeling preferential flow in an intermittent flood-irrigated field. Water Resour. Res. 33, 2049–2063.

Mohanty, B.P., Bowman, R.S., Hendrickx, J.M.H., Simunek, J., van Genuchten, M.Th., 1998. Preferential transport of nitrate to a tile drain in an intermittent-flood-irrigated field: Model development and experimental evaluation. Water Resour. Res. 34, 1061–1076.

Mualem, Y., 1976. A new model for predicting the hydraulic conductivity of unsaturated porous media. Water Resour. Res. 12, 513–522.

Oosterbaan, R.J., Pissarra, A., van Alphen, J.G., 1989. Hydraulic head and discharge relations of pipe drainage systems with entrance resistance. p. 86-98. In Proceedings of 15th European Regional Conference on Agricultural Water Management. Vol. III ICID, Dubrovnik.

Richard, T.L., Steenhuis, T.S., 1988. Tile drain sampling of preferential flow on a field scale. J. Contam. Hydrol. 3, 307–325.

Simunek, J., Vogel, T., van Genuchten, M.Th., 1994. The SWMS_2D Code for simulating water flow and solute transport in tow dimensional variably saturated media (Version 1.21). Research Report No. 132. U.S. Salinity Laboratory Agricultural Research Service, U.S. Department of Agriculture, Riverside, California.

Stamm, C., 1997. Rapid transport of phosphorus in drained grassland soils. PhD Dissertation No. 12486, Swiss Federal Institute of Technology Zürich.

Stuyt, L.C.P.M., Dierickx, W., Martinez Beltran, J., 2000. Materials for subsurface land drainage systems. FAO Irrigation and Drainage Paper 60, Rome, Italy.

van Genuchten, M.Th., 1980. A closed-form equation for predicting the hydraulic conductivity of unsaturated soils. Soil Sci. Soc. Am. J. 44, 892–898.

van Genuchten, M.Th., Wierenga, P.J., 1976. Mass transfer in sorbing porous media. I: Analytical solutions. Soil Sci. Soc. of Am. J. 40, 473–480.

van Genuchten, M.Th., Sudicky, E.A., 1999. Recent advances in vadose zone flow and transport modeling. In: Parlange, M.B., Hopmans, J.W. (Eds.). Vadose Zone Hydrology: Cutting Across Disciplines. Oxford University Press, New York, pp. 155–193.

Vogel, T., Huang, K., Zhang, R., Van Genuchten, M. Th., 1996. The HYDRUS code for simulating one-dimensional water flow, solute transport, and heat movement in variable-saturated media, version 5. U.S. Salinity Laboratory, ARS, Riverside, California.

Youngs, E.G., 1980. The analysis of groundwater seepage in heterogeneous aquifers. Hydrol. Sci. Bull. 25, 155–165.